Thermochimica Acta, 55 (1982) 97–111
Elsevier Scientific Publishing Company, Amsterdam—Printed in The Netherlands

EFFECT OF EXPERIMENTAL PARAMETERS ON NON-ISOTHERMAL TG

A.K. LAHIRI

Department of Metallurgy, Indian Institute of Science, Bangalore 560 012 (India)

H.S. RAY

Department of Metallurgical Engineering, Indian Institute of Technology, Kharagpur 721 302 (India)

(Received 9 November 1981)

ABSTRACT

The effect of some experimental parameters, namely sample weight, particle size and its distribution, heating rate and flow rate of inert gas, on the fractional decomposition of calcium carbonate samples have been studied both experimentally and theoretically. The general conclusions obtained from theoretical analysis are corroborated qualitatively by the experimental data. The analysis indicates that the kinetic compensating effect may be partly due to the variations in experimental parameters for different experiments.

INTRODUCTION

Thermogravimetric (TG) data are generally analysed using the integrated form of the rate equation

$$d\alpha/dt = k(1-\alpha)^n \tag{1}$$

where α is the fractional reaction or decomposition at time t, k is the reaction rate constant and n is the order of reaction. In the case of non-isothermal studies with a constant rate of temperature rise, i.e., $dT/dt = B$, Coats and Redfern's integrated form of the rate equation [1]

$$g(\alpha) = \int_0^\alpha \frac{d\alpha}{(1-\alpha)^n} = \frac{ART^2}{BE}\left(1 - \frac{2RT}{E}\right) e^{-E/RT} \tag{2}$$

is mostly used to evaluate the frequency factor A and activation energy E of the reaction.

Recently, Lahiri [2] has shown that for a sample having wide particle size distribution, the analysis of TG data by eqn. (2) may lead to erroneous conclusions regarding the values of E and A. The analysis was made for a hypothetical and ideal zero concentration of product gas within the sample.

In actual TG studies, the sample is normally present in the sample holder in the form of a loosely packed bed. So, generally, the concentration of the product gas

0040-6031/82/0000–0000/$02.75

"G" of the reaction

$$S(s) = S'(s) + G(g) \tag{3}$$

may not be zero throughout the bed, even when experiments are conducted in vacuum or an inert atmosphere. In the present article, the effect of concentration gradient within the sample bed on the fractional decomposition has been analysed. This gradient is influenced by several experimental factors such as the flow rate of the gas, heating rates etc.

Let us assume that W g of sample having N size fractions is filled up to height L in the sample holder as shown in Fig. 1. Assuming that each particle in the sample decomposes according to reaction (3) in a topochemical fashion, the rate of decomposition of any particle can be expressed as

$$-\frac{d}{dt}\left(\frac{4}{3}\pi r_i^3 \rho\right) = 4\pi r_i^2 k'(C^e - C) \tag{4}$$

where r_i is the instantaneous radius of unreacted core at time t, ρ is the difference in the density of the reactant solid S and that of the product solid S', k' is apparent reaction rate constant, C^e is the equilibrium concentration of the product gas G at the solid/gas interface and C is the actual concentration of the product gas G in the bulk phase around the particle under consideration. The bulk concentration of G obviously changes with height. To evaluate the concentration of the product gas around any particle we first make the following simplifying assumptions.

(i) There is no temperature gradient within the sample bed.

(ii) The concentration of the product gas is a function of height, Z co-ordinate, only. That is, there is no radial gradient.

(iii) The size distribution of particles and the porosity of the bed are constant throughout the sample bed.

(iv) There is no accumulation of gas within the sample bed. For most of experimental conditions these assumptions should be reasonably valid.

The mass balance equation for product gas in the bed can be expressed in terms of the flux (J) of G, and the rate of the generation of G per unit volume of bed, $\dot{n}$, as [3]

$$-(dJ/dZ) + \dot{n} = 0 \tag{5}$$

where

$$J = -D^e(dC/dZ) \tag{6}$$

and D^e is the effective diffusivity of G in the bed. D^e is related to the molecular

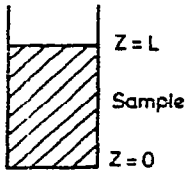

Fig. 1. Sample holder.

diffusivity of the gas, D^G by the relationship [3]

$$D^e = (\epsilon/\tau)D^G \tag{7}$$

where ϵ is the porosity of the sample bed and τ is the tortuosity factor.

With the progress of the reaction, finer particles will get completely reacted sooner. Therefore, the number of size fractions that will react at any instant of time will be $N' \leqslant N$. From eqn. (4) the rate of generation of G per unit bed volume

$$\dot{n} = \sum_{i=1}^{N'} n_i \frac{d}{dt}\left(\frac{4}{3}\pi r_i^3 \rho\right) = \sum_{i=1}^{N'} n_i 4\pi r_i^2 k'(C^e - C) \tag{8}$$

where n_i is the number of particles of ith size fraction per unit volume of the sample bed and r_i is the radius of unreacted core. In eqn. (8), the value of N' is determined by the condition

$$r_{N'+1} = 0;\ r_{N'} > 0 \tag{9}$$

The concentration C of the product gas in the bed can be expressed as

$$C = \frac{P}{RT} \tag{10}$$

where P is the partial pressure of the product gas G at any height in the bed, R is gas constant and T is the temperature of the bed. From eqns. (5), (6), (8) and (10)

$$D^e \frac{d^2P}{dZ^2} + \sum_{i=1}^{N'} 4\pi n_i r_i^2 k'(P^e - P) = 0 \tag{11}$$

where P^e is the equilibrium pressure of the product gas. Again, from eqns. (4) and (10), $(\partial r_i/\partial T)$ can be expressed as

$$-\frac{\partial r_i}{\partial T} = \frac{k'}{RTB\rho}(P^e - P) \tag{12}$$

where $B = (dT/dt)$, is the rate of temperature rise of the sample. The boundary conditions are

$$\text{at } T = 0,\ r_i = R_i \tag{13}$$

$$Z = 0,\ (dP/dZ) = 0 \tag{14}$$

$$Z = L,\ D^e(dP/dZ) = K_g(P - P^b) \tag{15}$$

where R_i is the radius of the ith size fraction particles, K_g is the mass transfer coefficient and P^b is the partial pressure of G outside the sample surface. Equation (14) implies that the bottom of the sample holder is impervious and eqn. (15) states that the amount of gas arriving at the sample surface is equal to the amount of the gas removed from the sample surface. The temperature dependence of k' and P^e are given by

$$k' = A'\, e^{-Q/RT} \tag{16}$$

$$P^e = \exp\left[-(\Delta H^0 - T\Delta S^0)/RT\right] \tag{17}$$

where A' and Q are respectively the apparent frequency factor and activation energy

for reaction (3) and ΔH^0 and ΔS^0 are the standard enthalpy and entropy changes respectively of reaction (3). It is well known that over a limited temperature range, D^G and hence D^e can be expressed as

$$D^e = D_0(T/T_0)^m \tag{18}$$

where m is a constant, and D_0 is the effective diffusivity at temperature T_0.

Since the mass transfer coefficient is directly proportional to D^G, K_g can be expressed as

$$K_g = K_g^0(T/T_0)^m \tag{19}$$

where K_g^0 is the mass transfer coefficient at T_0.

From eqns. (16)–(19) and eqns. (11)–(15) we obtain the following dimensionless equations

$$\frac{-\mathrm{d}^2 y}{\mathrm{d}\zeta^2} + D\frac{\mathrm{e}^{-Q/RT}}{(T/T_0)^m}\sum_{i=1}^{N'}\left(n_i' x_i^2\right) y = 0 \tag{20}$$

$$\frac{-\partial x_i}{\partial T} = b\frac{\mathrm{e}^{-(Q+\Delta H^0)/RT}}{T}\, y \tag{21}$$

$$\text{at } T = 0,\ x_i = x_i^0 \tag{22}$$

$$\zeta = 0,\ (\mathrm{d}y/\mathrm{d}\zeta) = 0 \tag{23}$$

$$\zeta = 1,\ (\mathrm{d}y/\mathrm{d}\zeta) = Sh\left(1 - \left(P^b/P^e\right) - y\right) \tag{24}$$

where the dimensionless height, ζ, dimensionless pressure, y, and the radius of the unreacted core of particles of ith size fraction x_i are given by

$$\zeta = Z/L \tag{25}$$

$$y = (P^e - P)/P^e \tag{26}$$

$$x_i = r_i/R_1 \tag{27}$$

the other dimensionless terms appearing in eqns. (20)–(24) are given by the following four equations

$$D = \left(4\pi L^2/D_0\right) n_1 R_1^2 A' \tag{28}$$

$$b = A'\,\mathrm{e}^{\Delta S^0/R}/RB\rho R_1 \tag{29}$$

$$Sh = K_g^0 L/D_0 \tag{30}$$

$$n_i' = n_i/n_1 \tag{31}$$

where n_1 is the number of particles of largest radius, R_1, per unit volume of the sample bed. The dimensionless term D, eqn. (28), is a measure of the ratio of diffusion resistance to resistance for the chemical reaction. Sh is the ratio of the diffusion resistance to mass transfer resistance. The term b defined by eqn. (29) can be considered as a dimensionless frequency factor for non-isothermal TG.

The fractional decomposition per unit bed volume, f, at any value of ζ and the

total (or observed) decomposition, are given by

$$f = 1 - \left(\sum_{i=1}^{N'} x_i^3 n_i' \Big/ \sum_{i=1}^{N} n_i' (x_i^0)^3 \right) \tag{32}$$

$$\alpha = \int_0^1 f d\zeta \tag{33}$$

where $x_i^0 = R_i/R_1$. The values of α and f can be obtained from eqns. (20)–(24), (32), (33) and the dimensionless form of eqn. (9) i.e.,

$$x_{N'+1} = 0, x_{N'} > 0 \tag{34}$$

RESULTS AND DISCUSSION

Results obtained from theory

The eqns. (20)–(24) along with eqn. (34) were solved by the orthogonal collocation method [4] (see appendix). All calculations were carried out using $Q = 14$ kcal g mole^{-1}, $\Delta H^0 = 40.2$ kcal g mole^{-1}, $P^b = 0$ and $m = 1.6$. Analysis of experimental data for calcium carbonate decomposition, reported later, by eqn. (2) leads to an average value for E of about 54 kcal g mole^{-1}. Since $E \simeq \Delta H^0 + Q$, and ΔH^0 for the decomposition of $CaCO_3$ is 40.2, Q was assumed to be 14 kcal g mole^{-1}. Figure 2 shows the concentration profile of the product gas in the sample bed. The concentration of the product gas is maximum at $\zeta = 0$ minimum y, and minimum at $\zeta = 1$. It is apparent that the concentration profile is strongly dependent on the value of D. Figure 3 shows the variation of fractional decomposition, f, along the height of the

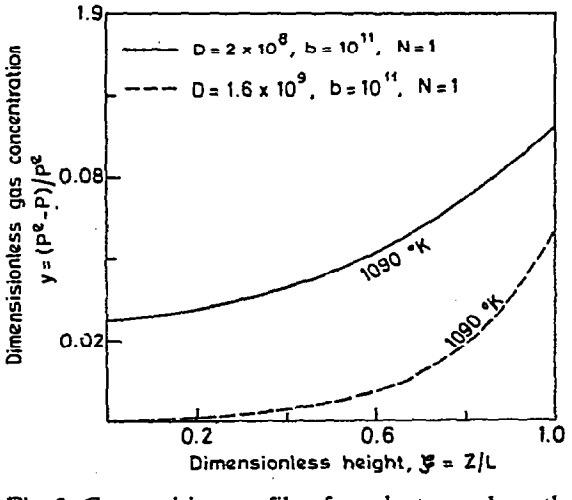

Fig. 2. Composition profile of product gas along the height of the sample bed.

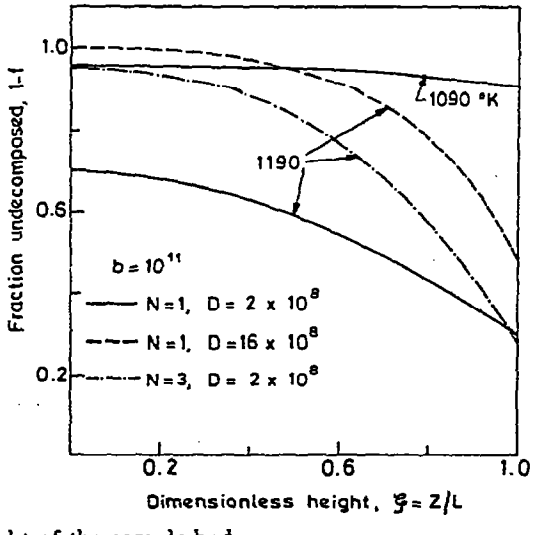

Fig. 3. Profile of fractional decomposition along the height of the sample bed.

bed. Low fractional decomposition at $\zeta = 0$, is due to the low value of the driving force of decomposition y. Figure 4 shows the effect of D, b and Sh on the total or observed fractional decomposition. It is interesting to note that even when the fractional decomposition varies along the height of the sample bed, $\ln\{g(\alpha)/T^2\}$ is approximately linearly related to $1/T$. Furthermore the slopes of the lines are not very sensitive to the values of D, b and Sh. The activation energy calculated from the slopes of the curves in Fig. 4 vary between 44 and 55 kcal g mole^{-1}.

Figure 4 shows that the overall reaction rate is strongly dependent on D and Sh, when the value of D is large. However, the effect of both D and Sh become insignificant when the value of D is small. An approximate idea of the value of D where it will strongly influence the observed rate can be obtained as follows.

Assuming $\Sigma_{i=1}^{N'}(n_i' x_i^2)$ is independent of ζ, the solution of eqn. (20) for the boundary conditions given by eqns. (23) and (24) is

$$y = \frac{Sh(1 - P^b/P^c)}{u \sinh(u) + Sh \cosh(u)} \cosh(u\zeta) \tag{35}$$

where

$$u = \left\{ \frac{D\, e^{-Q/RT}}{(T/T_0)^m} \sum_{i=1}^{N'} (n_i' x_i^2) \right\}^{1/2} \tag{36}$$

When $u \ll 1$; eqn. (35) reduces to

$$y = \frac{Sh(1 - P^b/P^c)}{u^2 + Sh} \tag{37}$$

If $Sh \gg u$ which is expected to be valid when $u \ll 1$, eqn. (37) simplifies to

$$y = 1 - P^b/P^c \tag{38}$$

In other words when $u \ll 1$, the composition of the product gas will be uniform throughout the bed. On the other hand, when $u \gg Sh$, eqn. (35) reduces to

$$y \simeq 0 \tag{39}$$

which indicates that the reaction rate will be practically zero. Thence, the composition profile of the product gas and hence the observed rate of decomposition will be very sensitive to the diffusion resistance offered by the sample bed, D, when u is of the order of unity. Since u, eqn. (36), is strongly temperature dependent, u may be much less than unity at low temperatures but it may become quite significant at high temperatures.

The preceding discussion shows that the concentration of the product gas within the sample bed will be the same as that above the bed only when the sample size is such that over the entire temperature range under investigation the value of u is much less than unity. Under this condition, for uniform particle size, the activation energy calculated from the plot of $\ln\{g(\alpha)/T^2\}$vs. $1/T$ leads to a correct value of the activation energy for the reaction. In Fig. 4 for curve IV, $u \ll 1$, and the activation energy obtained from the slope is 55 which compares well with the actual value used for calculation, $54.2(Q + \Delta H^0)$.

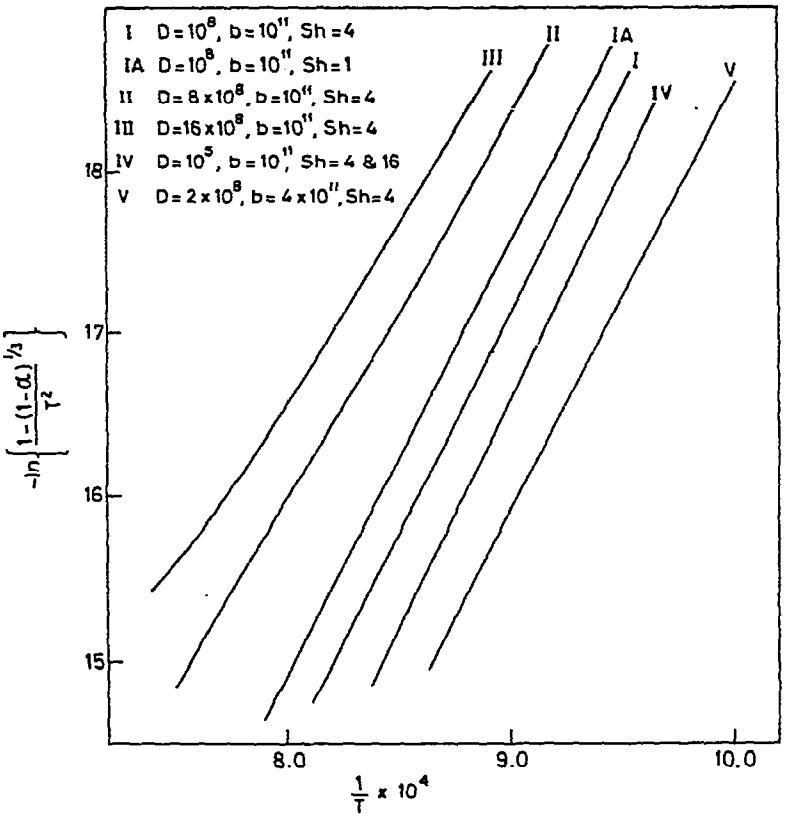

Fig. 4. Effect of D, b, and Sh on the fractional decomposition for the uniform particle size, $N = 1$.

As long as the condition $u \ll 1$ is satisfied over the temperature range under investigation, any change of D or Sh will not alter the fractional decomposition rate. On the other hand, if under the experimental conditions u is not very small, any change in the experimental condition will alter the rate of fractional decomposition.

Figure 5 shows the effect of particle size distribution on the calculated fractional decomposition rate when the relative amount of various size fractions are the same and $R_i/R_{i-1} = \sqrt{2}$. It is apparent that the slope of $\ln\{g(\alpha)/T^2\}$ vs. $1/T$ plot is not very sensitive to the size distribution of particles when D is very large. On the other hand, when D is relatively small, wide size distribution may lead to significant non-linearity of the plot. Furthermore for the constant values of D, b and Sh, the reaction rate decreases with the increase in the number of size fractions in the sample. Figure 6 shows the plot of E vs. $\log(AR/B)$ calculated for the curves presented in Figs. 4 and 5. In spite of considerable scatter of the data points a linear relationship is apparent. This suggests that the kinetic compensating effect may be partly due to the variation of the experimental parameters.

Experimental results

The effect of various experimental parameters on the fractional decomposition rate of a high grade commercial limestone (CaO 99.5%) was studied using a Stanton

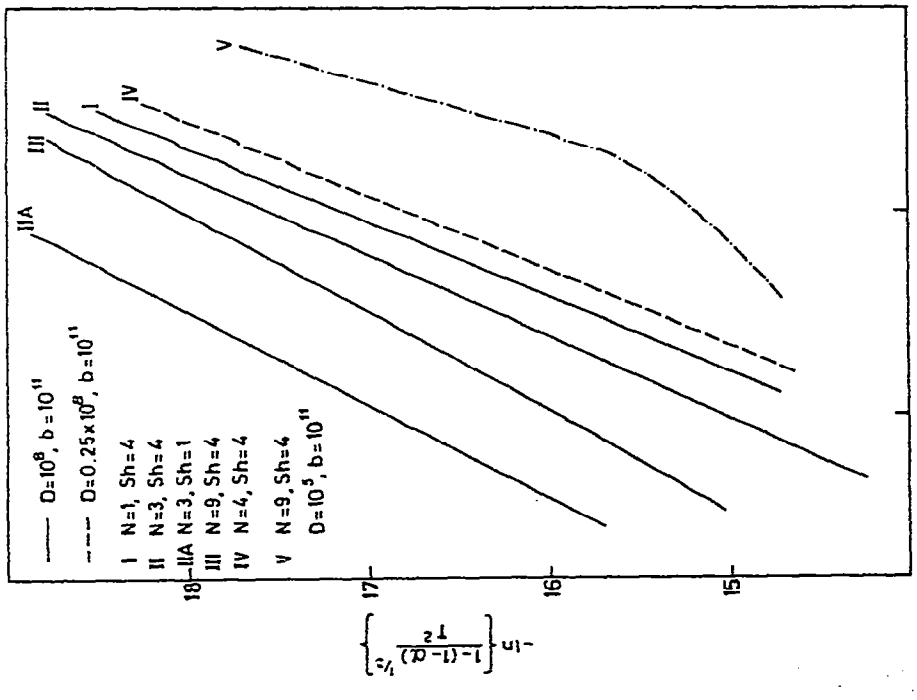

Fig. 5. Effect of particle size distribution on the fractional decomposition.

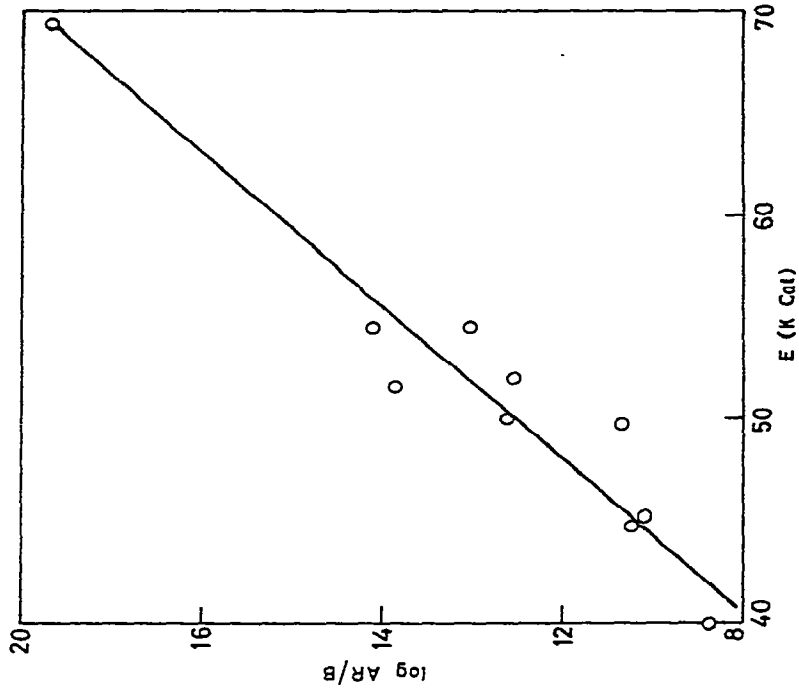

Fig. 6. Kinetic compensating effect.

Redcroft TG apparatus (model-770). All experiments were carried out in a flowing stream of nitrogen.

Experimental parameters were varied one at a time. The thermobalance gives continuous plots during weight loss runs. The figures shown subsequently show some actual data points. Figure 7 shows the effect of sample weight on the decomposition rate. Increase in sample weight increases the height of the sample bed, L. Thereby both D and Sh increase, the increase in the former being much more than in the latter. Curves in Fig. 4 indicate that this will lead to a decrease in the fractional reduction rate which is in agreement with Fig. 7. Figure 8 shows the effect of the addition of inert diluent Al_2O_3 and the packing of the bed. For uniformly sized particles, the number of $CaCO_3$ particles per unit sample bed volume, n, and height

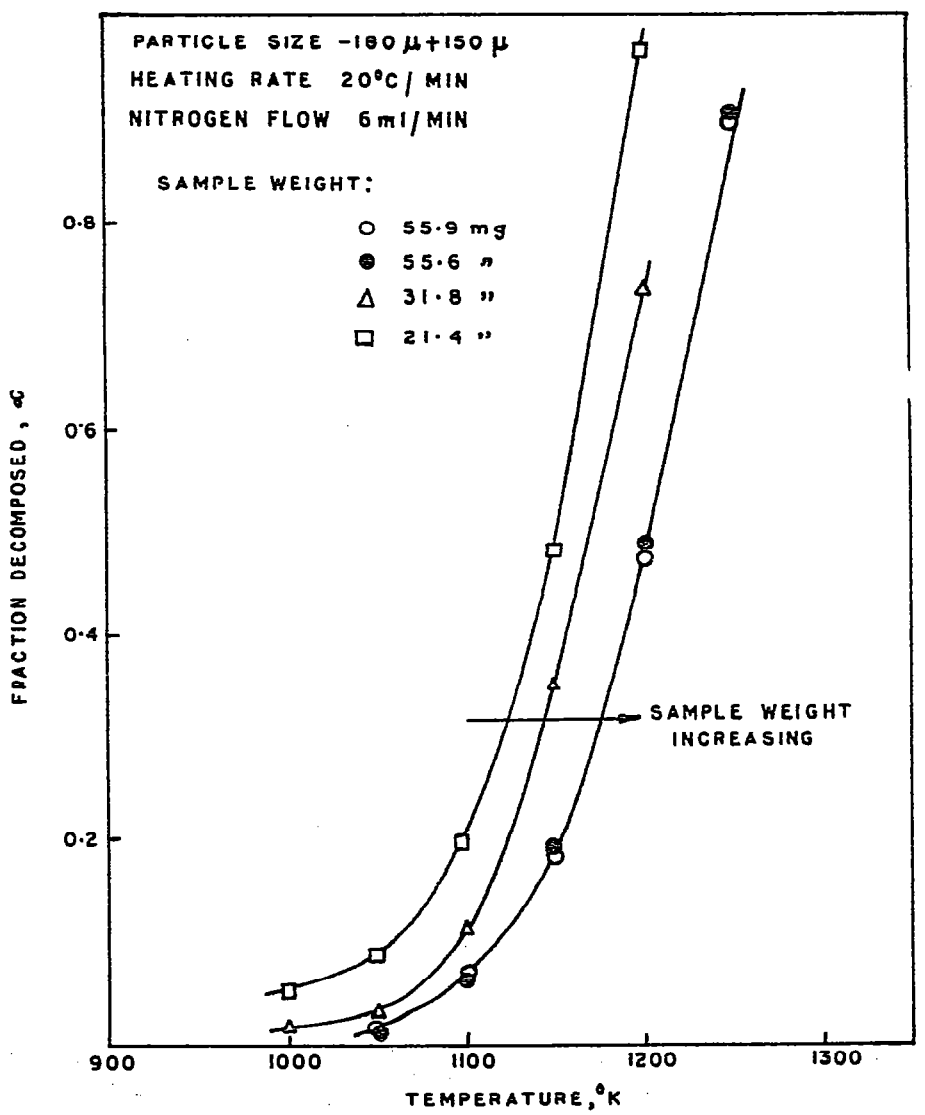

Fig. 7. Effect of sample weight on decomposition rate.

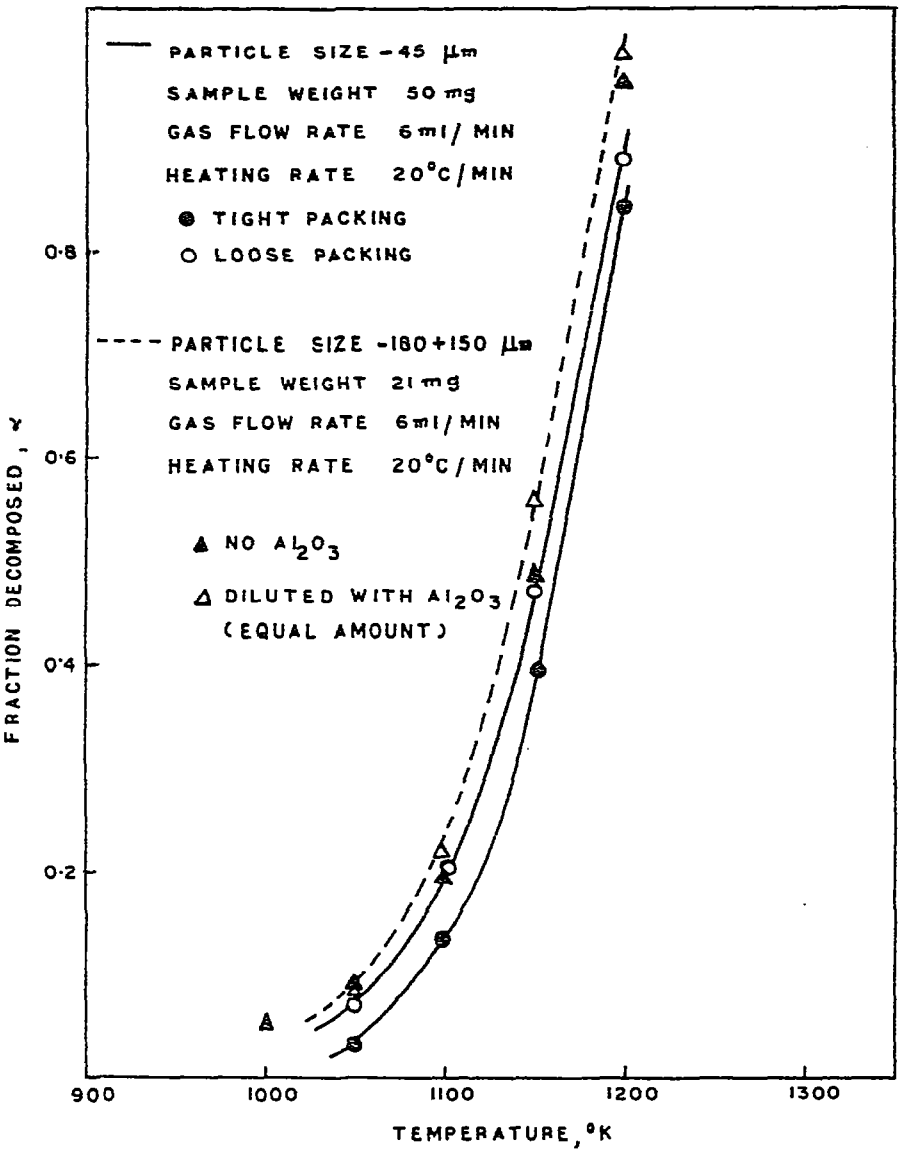

Fig. 8. Effect of Al_2O_3 dilution and of compaction on decomposition rate.

of the sample bed can be expressed as

$$n = n_1 = \frac{1-\epsilon}{\frac{4}{3}\pi R_1^3} \frac{V}{V+V'} \tag{40}$$

$$L = \frac{V+V'}{S(1-\epsilon)} \tag{41}$$

where V and V' are the volumes of $CaCO_3$ and Al_2O_3, respectively, and S is the area of the base of the sample holder. Equations (40) and (41) suggest that the addition of inert diluent will reduce n_1 and increase L but the product $(n_1 L)$ will remain

unchanged. Thereby the addition of the inert diluent will increase D, eqn. (28), and Sh, eqn. (30), by the same amount. Figure 4 shows that when the observed fractional decomposition rate is sensitive to the value of D, the effect of an increase in D and Sh on the fractional decomposition rate are almost of the same order of magnitude but of opposite sign. Thereby the addition of Al_2O_3 to the sample does not alter the fractional decomposition rate. On the other hand the packing of the bed reduces the porosity of the bed ϵ. Equations (40) and (41) suggest that the product $(n_1 L)$ is independent of porosity but L decreases with a decrease in porosity. Since effective diffusivity, D^e, eqn. (7), is directly proportional to ϵ, it can be shown that

$$D \propto (1-\epsilon)/\epsilon \tag{42}$$

Thereby dense packing of the bed will increase D and reduce Sh resulting in a decrease in the fractional decomposition rate.

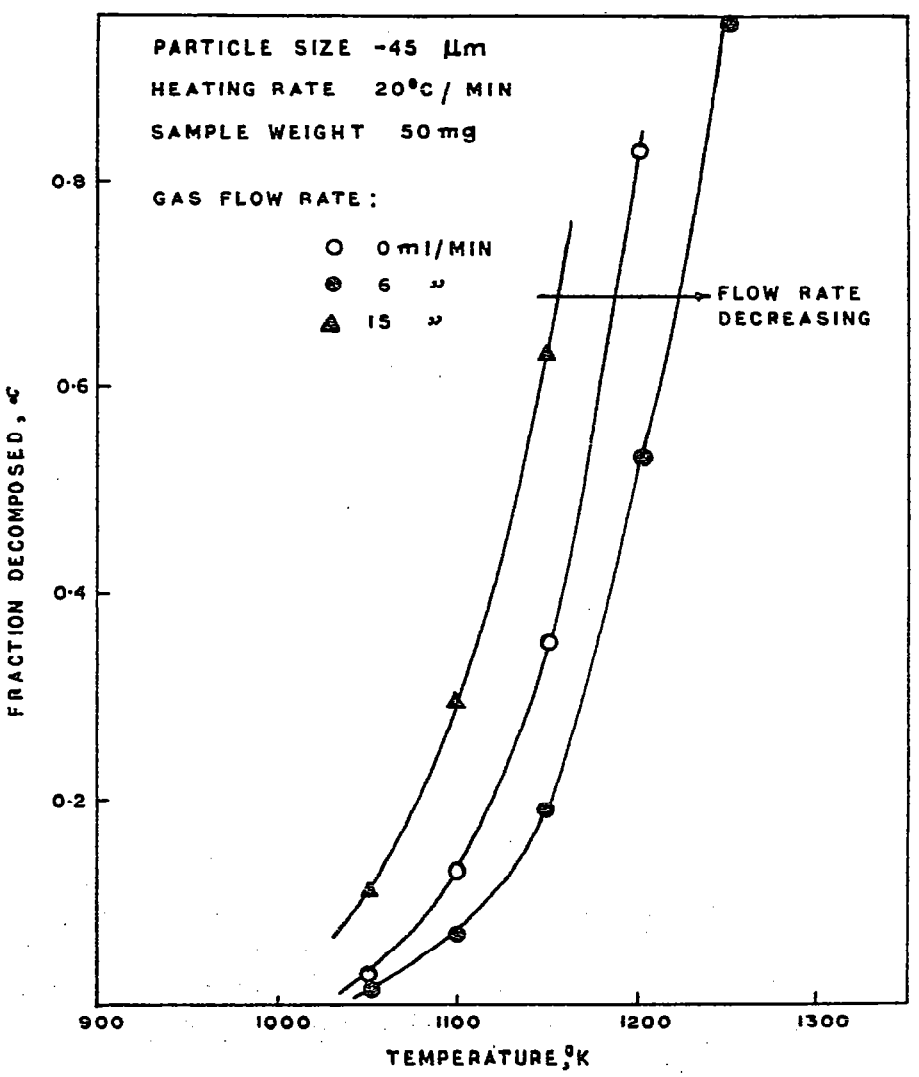

Fig. 9. Effect of gas flow rate on decomposition rate.

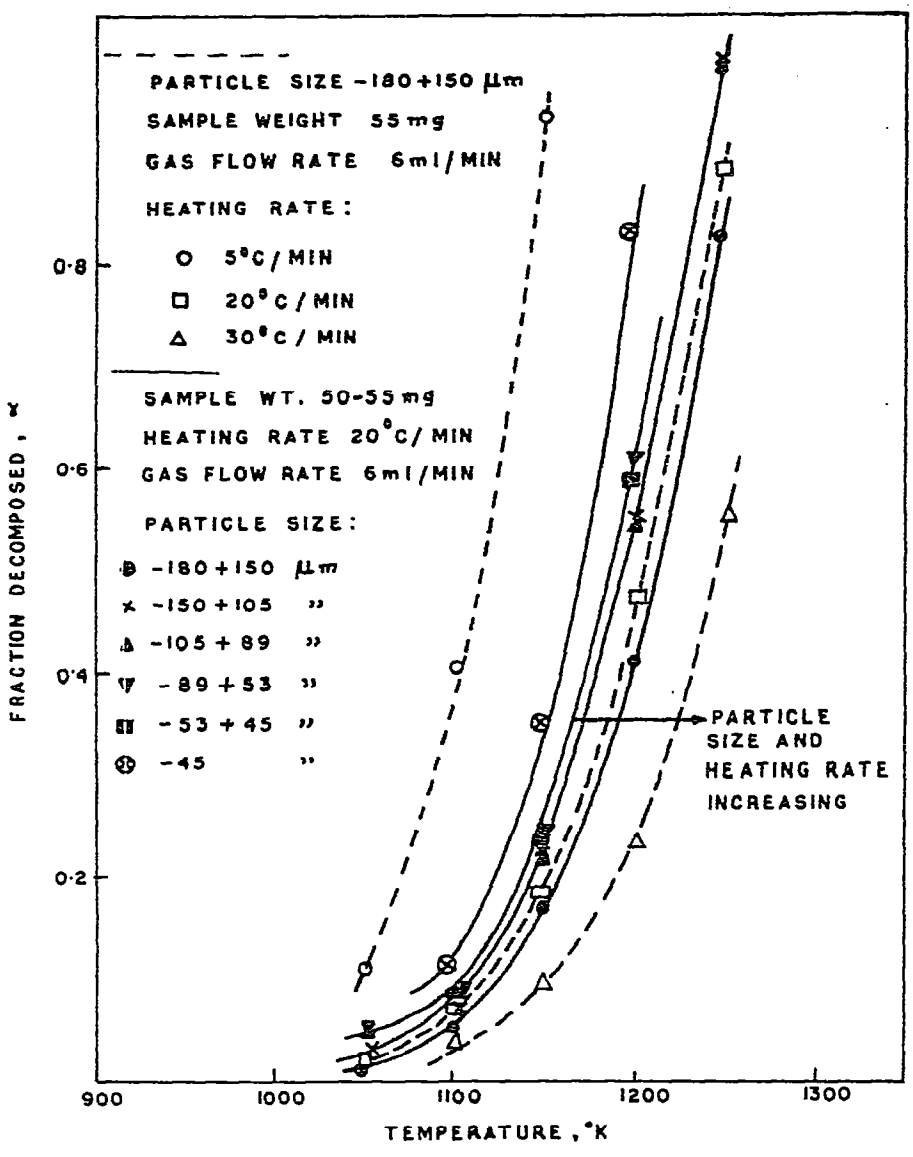

Fig. 10. Effect of particle size and heating rate on decomposition rate.

The effect of gas flow rate is shown in Fig. 9. Increase in gas flow rate increases the mass transfer coefficient K_g and hence Sh, resulting in an increase in the decomposition rate.

Figure 10 shows the effect of particle size and heating rate when these parameters are varied individually. Increase in the heating rate decreases the value of b, eqn. (29), and hence decreases the decomposition rate. Equation (40) shows that for uniformly sized particles $n_1 R_1^2$ is inversely proportional to R_1. So a reduction in particle size will increase both D and b by the same factor. Figure 4 shows that the fractional decomposition rate is more sensitive to b, hence a decrease in particle size results in an increase in the decomposition rate.

Figure 11 shows the effect of particle size distribution on the fractional decom-

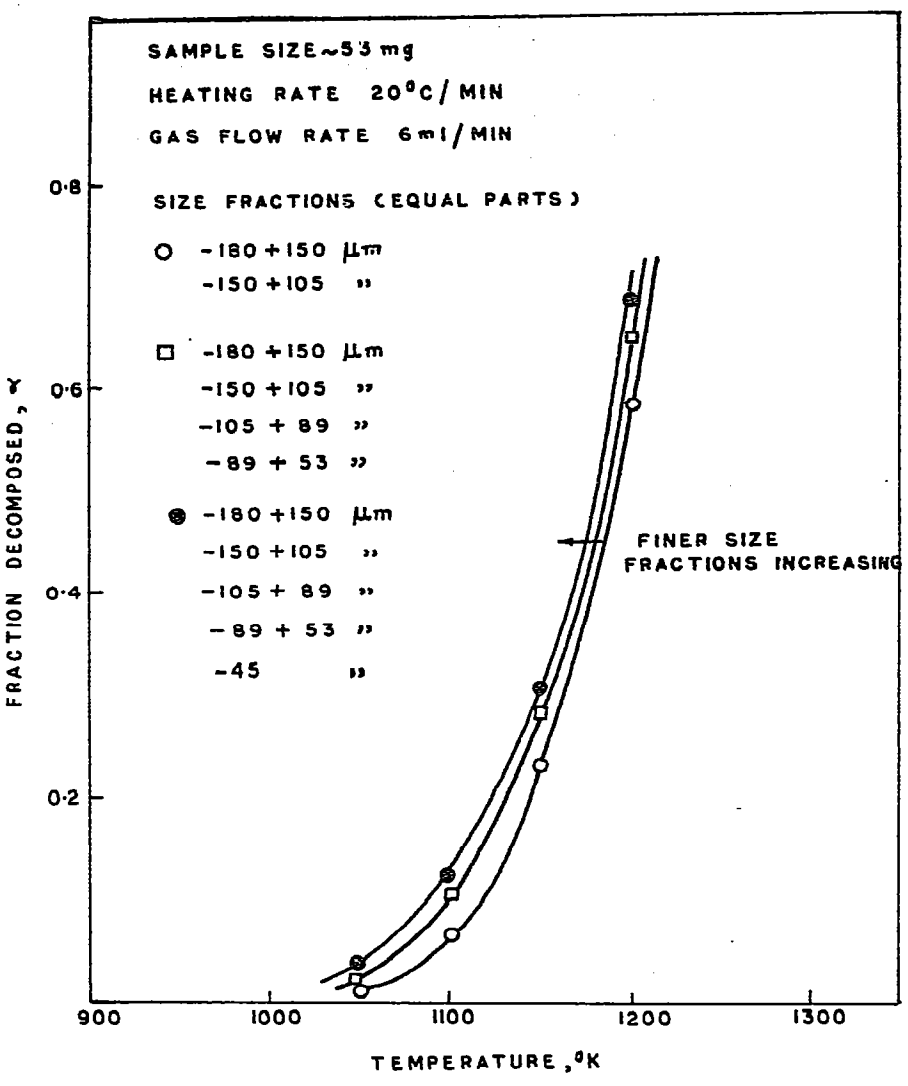

Fig. 11. Effect of particle size distribution on decomposition rate.

position rate. These experiments were carried out using almost the same total weight of the sample in each case and mixing equal proportions of various size fractions. The average size of the largest particles was the same ($-180\ \mu m + 150\ \mu m$) for all the experiments. It can be shown that, for the above mentioned condition, the number of largest particles n_1 and hence D are inversely proportional to the number of size fractions in the sample, N. Curves I and IV in Fig. 5 indicate that the net effect of the increase in the number of size fractions in the sample is a slight increase in the fractional decomposition rate. This is in agreement with the experimental data shown in Fig. 11.

The values of $\ln\{g(\alpha)/T^2\}$ for the data points shown in Figs. 7–11 yield linear plots when plotted against $1/T$.

Figure 12 shows the plot of E vs. $\log AR/B$ obtained from the experimental data. A linear relationship is apparent from the figure. Both Figs. 6 and 12 indicate that

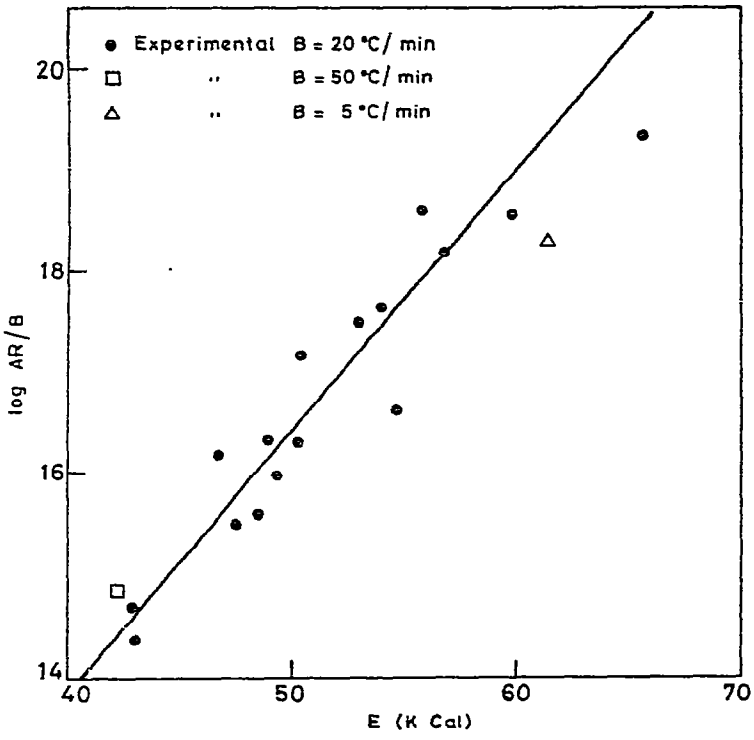

Fig. 12. Kinetic compensating effect.

the kinetic compensating effect may be partly due to the variation in experimental parameters for different experiments.

ACKNOWLEDGEMENT

The experimental work was carried out by one of the authors (H.S.R.) at Pilkington Brothers Limited, Lathom, Lancs, U.K. He is grateful for permission to use the thermobalance.

REFERENCES

1 A.W. Coats and J.P. Redfern, Nature, 201 (1964) 68.
2 A.K. Lahiri, Thermochim. Acta, 40 (1980) 289.
3 J. Szekeley and N.J. Themlis, Rate Phenomena in Process Metallurgy, Wiley Interscience, New York, 1971.
4 B.A. Finlayson, The Methods of Weighted Residuals and Variational Principles, Academic Press, New York, 1972.

APPENDIX

Orthogonal collocation method

To solve eqns. (20)–(24), it was assumed that y can be represented by

$$y = A\cosh(\beta_0\zeta) + \sum_{j=0}^{l} a_j\zeta^j \tag{A1}$$

where

$$\beta_0 = \left\{\frac{D}{(T/T_0)^m}\, e^{-Q/RT}\sum_{i=1}^{N'} n_i' x_i^2\right\}_{\zeta=0}^{1/2} \tag{A2}$$

A, a_js are unknown functions of T and l is the maximum order of the polynomial. The boundary condition eqn. (23) suggests a_1 must be zero. Substituting eqn. (A1) in eqns. (20), (24) and (21)

$$(\beta - \beta_0^2)A\cosh(\beta_0\zeta) + \beta a_0 + \sum_{j=2}^{l} a_j\{-j(j-1)\zeta^{j-2} + \beta\zeta^j\} = 0 \tag{A3}$$

$$A\{\beta_0\sinh\beta_0 + Sh\cosh\beta_0\} + Sh\, a_0 + \sum_{j=2}^{l} a_j(j+Sh) = Sh\frac{(1-P^b)}{P^c} \tag{A4}$$

where

$$\beta = \frac{D}{(T/T_0)^m}\, e^{-Q/RT}\sum_{i=1}^{N'} n_i' x_i^2 \tag{A5}$$

and

$$-\frac{\partial x_i}{\partial T} = \frac{b\, e^{-(Q+\Delta H^0)/RT}}{T}\left\{A\cosh(\beta_0\zeta) + \sum_{j=2}^{l} a_j\zeta^j\right\} \tag{A6}$$

For an lth order polynomial $a_1, a_2 \ldots a_l$ were evaluated by satisfying eqn. (A3) at the roots of an lth order Legendre polynomial [4]. The eqns. (A3)–(A6) were solved simultaneously along with the initial condition eqn. (22). In all cases the required degree of accuracy, difference between the calculated values of fractional decomposition for two successive degrees of polynomial less than 0.1%, could be obtained for $l \leqslant 6$.